AIAS 2015 - 562

DEVELOPMENT AND VALIDATION OF NUMERICAL TOOLS FOR FSI ANALYSIS AND STRUCTURAL OPTIMIZATION: THE EU "RIBES" PROJECT STATUS

Ubaldo Cella[a], Marco Evangelos Biancolini[b], Corrado Groth[b], Andrea Chiappa[b], Domiziano Beltramme[b]

[a] *Design Methods - Aerospace engineering consulting company (www.designmethods.aero), Viale Regina Elena 207, 98121 Messina, e-mail: ubaldo.cella@designmethods.aero*
[b] *Università di Roma "Tor Vergata" - Dipartimento di Ingegneria dell'Impresa "Mario Lucertini", Via del Politecnico 1, 00133 Roma, e-mail: biancolini@ing.uniroma2.it*

Sommario
Una strategia comunemente adottata per modellare il meccanismo di interazione Fluido-Struttura (FSI) consiste nell'accoppiare la soluzione fluidodinamica, ottenuta con metodi basati sulla CFD, a solutori strutturali in un processo iterativo. Il progetto di ricerca europeo "RIBES", finanziato nell'ambito del settimo programma quadro (aeronautica e trasporto aereo), è finalizzato all'incremento dell'accuratezza di strumenti di analisi aeroelastica basati sull'accoppiamento CFD-CSM, allo sviluppo di ambienti di ottimizzazione strutturale e alla definizione di una campagna sperimentale di prove aeroelastiche in galleria del vento per la validazione di codici di analisi aeroelastica. Lo strumento matematico sul quale si basa la strategia di parametrizzazione delle geometrie e la tecnica di interpolazione adottata nella procedura di trasferimento dei carichi fra il dominio fluidodinamico e quello strutturale, fa riferimento alle Radial Basis Functions. Questo documento fornisce una panoramica del progetto RIBES, ne riporta lo stato delle attività e descrive la pianificazione della campagna sperimentale.

Abstract
A common strategy to model the Fluid Structure Interaction (FSI) mechanisms is to couple the fluid dynamic solution, obtained by CFD tools, with structural solvers in an iterative process. The European "RIBES" research project, funded within the 7th framework programme (aeronautics and air transport), is focused on the improvement of the accuracy of CFD-CSM based aeroelastic analysis tools, on the development of structural optimization environments and on the setup of an aeroelastic wind tunnel test campaign aimed to the FSI analysis codes validation. The shape parameterization strategy and the interpolation technique adopted in the loads transfer procedure between CFD and FEM domains are based on the Radial Basis Functions mathematical framework. An overview of the RIBES project, a report on the status of its activities and the description of the experimental campaign plan are in this paper provided.

Keywords: Aeroelasticity, Fluid Structure Interaction, load mapping, Computational Fluid Dynamic, Radial Basis Functions.

1. INTRODUCTION

The capability to model the interaction of the several mechanisms involved in physics phenomena represents a key point in the development of efficient tools for engineering design. Furthermore, the interest in automating the procedure able to face such analyses raised with the modern view of facing design problems by numerical optimization strategies. The importance of such approach is particularly felt in the aerospace sector where the integration of multidisciplinary numerical analysis methods within optimization environments became a standard approach in many design processes.

A discipline on which large research efforts were addressed, in the last decades, is Aeroelasticity[1]. The interaction between aerodynamic loads and structural deformations is, in fact, often the predominant mechanism to which the aircraft aerodynamic designer has to deal with. The aerodynamic loads induce a deformation that, in a closed loop, and have impact on aerodynamics according to the structural properties of the object involved in the fluid interaction. It is then clear how the capability to include the structural aeroelastic response in the shape design process is strategic in improving the ability to produce lighter, greener and cheaper aircrafts.
One of the most common and accurate strategies to model the Fluid Structure Interaction (FSI) mechanisms is to couple RANS (Reynolds-averaged Navier-Stokes) solvers, with Finite Element codes in a so called CFD-CSM (Computational Fluid Dynamics - Computational Structural Mechanics) coupling procedure. Several complexities are related to the implementation of such technologies. One of them concerns the technique with which to transfer the aerodynamic loads from the wet surfaces of the CFD mesh to the structural domain which, in general, have a non-conformal discretization on the common boundaries. The forces computed by the fluid dynamic analysis are, in fact, extracted from the cells of the CFD walls boundaries in the form of vectors positioned on a cloud of points that will typically differ from the FEM grid points on which the loads have to be applied (the grid requirements are, in general, different for FEM and CFD analyses). An interpolation between the two domains is then required with a consequential introduction of an error. The minimization of the uncertainness associated to this process relates to the quality of the mathematical approach with which to face the interpolation. The analysis automation and the implementation in optimization environments represent the closure of the MDO (Multidisciplinary Design Optimization) tool development problem.
FSI methodologies, as well as any numerical model, need to be validated against experiments. The availability of appropriate experimental databases on test cases representative of the typical phenomenon that the numerical tools are aimed to model, is another crucial aspect of the development process. A set of experimental static and dynamic aeroelastic campaigns have been planned in the past for codes validation purposes and made available to the scientific community (Agard 445.6, HIRENASD, EuRAM). Customized measurements are, however, often necessary to better meet the validation requirements.
The above cited topics are the central subjects of the "RIBES" European research project. The specific goals are the development of an accurate loads transfer procedure between fluid and structural domains, the implementation of a structural numerical optimization procedure and the setup of an experimental wind tunnel campaign aimed to the validation of the numerical tools. The innovative aspects of the research are the load mapping implementation procedure and the adoption of a mesh morphing technique, for the shape optimization, basing both on the Radial Basis Function (RBF) mathematical framework. RBFs have been also used in developing a Response Surface metamodel to be applied in the optimization procedure.
The other high valuable part of the project consist in allocating a significant part of the resources on the setup of an extensive aeroelastic wind tunnel test campaign to be performed on a model that replicates a typical metallic aeronautical wing structure. The aim is to generate an experimental base of assessment strongly customized to the software developed within the projects.
This paper provides an overview of the RIBES project, describes the experimental campaign, and reports the activities on progress.

2. THE RIBES PROJECT

The "RIBES" (Radial basis functions at fluid Interface Boundaries to Envelope flow results for advanced Structural analysis) project is led by the University of Rome "Tor Vergata" and is funded within the EU 7th framework aeronautics programme JTI-CS-GRA (Joint Technology Initiatives - Clean Sky - Green Regional Aircraft). The programme is aimed to the enhancement of numerical methodologies to shorten the time to market for new and cleaner solutions thus contributing to reduce the environmental impact of aviation (i.e. emissions and noise reduction but also green life cycle). The project started in December

[1] Aeroelasticity is involved in several EU projects with focus ranging from flow control to dynamic response (AFLoNext, SimSAC, 3AS, JTI Clean Sky).

2014 and has a duration of 18 months. As stated its scope is the development and validation of software tools for the accurate transfer of loads between numerical models and for structural shape optimization. It is divided into three main topics:

- Development of a load mapping procedure
- Development of a structural optimization procedure
- Setup of an experimental campaign

Partners of research are the **RBF Morph™** (www.rbf-morph.com) software vendor, whose technology is at the base of the implemented load mapping and shape parameterization methodologies, and the aerospace consulting engineering firm **Design Methods™** (www.designmethods.aero) which supports the activities related to aeronautics.

3. RECALLS OF RBF THEORY

Radial basis are very powerful tool able to interpolate everywhere in the space a function defined at discrete points from the exact value at original points. The behaviour of the function between points depends on the kind of basis adopted. The radial function can be fully or compactly supported. Typical RBF functions are shown in Table 1. RBFs are scalar functions with the scalar variable r, which is the Euclidean norm of the distance between two points defined in a generic n-dimensional space. In any case, a polynomial corrector is added to guarantee compatibility for rigid modes.

Table 1: Typical RBF functions

Radial Basis Functions with global support	$\varphi(r), r = \|r\|$	**Radial Basis Functions with compact support**	$\varphi(r) = f(\xi), \xi \leq 1, \xi = \frac{r}{R_{sup}}$
Spline type (R_n)	$r^n, n\ odd$	Wendland (C^0)	$(1-\xi)^2$
Thin plate spline (TPS_n)	$r^n \log(r), n\ even$	Wendland (C^2)	$(1-\xi)^4(4\xi+1)$
Multiquadric (MQ)	$\sqrt{1+r^2}$	Wendland (C^4)	$(1-\xi)^6\left(\frac{35}{3}\xi^2+6\xi+1\right)$

A linear system (of order equal to the number of source point introduced) needs to be solved for coefficients calculation. Once the unknown coefficients are calculated, the motion of an arbitrary point inside or outside the domain (interpolation/extrapolation) is expressed as the summation of the radial contribution of each source point (if the point falls inside the influence domain).
An interpolation function s composed by a radial basis φ and a polynomial h of order $m-1$, where m is said to be the order of φ, introduced with the aim to guarantee the compatibility for rigid motions, is defined as follows if N is the total number of contributing source points.

$$s(\boldsymbol{x}) = \sum_{i=1}^{N} \gamma_i \varphi\left(\left\|\boldsymbol{x} - \boldsymbol{x}_{\boldsymbol{k}_i}\right\|\right) + h(\boldsymbol{x}) \tag{1}$$

The degree of the polynomial has to be chosen depending on the kind of radial function adopted. A radial basis fit exists if the coefficients γ_i and the weight of the polynomial can be found such that the desired function values are obtained at source points and the polynomial terms give zero contributions at source points, that is:

$$s\left(\boldsymbol{x}_{\boldsymbol{k}_i}\right) = \boldsymbol{g}_i, 1 \leq i \leq N \tag{2}$$

$$\sum_{i=1}^{N} \gamma_i p\left(\boldsymbol{x}_{\boldsymbol{k}_i}\right) = 0 \tag{3}$$

for all polynomials p with a degree less or equal than that of polynomial h. The minimal degree of polynomial h depends on the choice of the basis function. A unique interpolator exists if the basis

function is a conditionally positive definite function [1]. If the basis functions are conditionally positive definite of order $m \leq 2$ [2], a linear polynomial can be used:

$$h(\boldsymbol{x}) = \beta_1 + \beta_2 x + \beta_3 y + \beta_4 z \tag{4}$$

The subsequent exposition assumes that the aforementioned hypothesis is valid. A consequence of using a linear polynomial is that rigid body translations are exactly recovered. The values for the coefficients γ of RBF and the coefficients β of the linear polynomial can be obtained by solving the system:

$$\begin{pmatrix} M & P \\ P^T & 0 \end{pmatrix} \begin{pmatrix} \gamma \\ \beta \end{pmatrix} = \begin{pmatrix} g \\ 0 \end{pmatrix} \tag{5}$$

where g are the known values at the source points. M is the interpolation matrix defined calculating all the radial interactions between source points:

$$M_{ij} = \varphi\left(\left\|\boldsymbol{x}_{\boldsymbol{k}_i} - \boldsymbol{x}_{\boldsymbol{k}_j}\right\|\right), 1 \leq i \leq N, 1 \leq j \leq N \tag{6}$$

and P is a constraint matrix that arises balancing the polynomial contribution and contains a column of "1" and the $\boldsymbol{x}\ \boldsymbol{y}\ \boldsymbol{z}$ positions of source points in the others three columns:

$$\boldsymbol{P} = \begin{pmatrix} 1 & x_{k_1} & y_{k_1} & z_{k_1} \\ 1 & x_{k_2} & y_{k_2} & z_{k_2} \\ \vdots & \vdots & \vdots & \vdots \\ 1 & x_{k_N} & y_{k_N} & z_{k_N} \end{pmatrix} \tag{7}$$

Radial basis interpolation works for scalar fields. For the smoothing problem, each component of the displacement field prescribed at the source points is interpolated as follows:

$$\begin{cases} s_x(\boldsymbol{x}) = \sum_{i=1}^{N} \gamma_i^x \varphi\left(\left\|\boldsymbol{x} - \boldsymbol{x}_{\boldsymbol{k}_i}\right\|\right) + \beta_1^x + \beta_2^x x + \beta_3^x y + \beta_4^x z \\ s_y(\boldsymbol{x}) = \sum_{i=1}^{N} \gamma_i^y \varphi\left(\left\|\boldsymbol{x} - \boldsymbol{x}_{\boldsymbol{k}_i}\right\|\right) + \beta_1^y + \beta_2^y x + \beta_3^y y + \beta_4^y z \\ s_z(\boldsymbol{x}) = \sum_{i=1}^{N} \gamma_i^z \varphi\left(\left\|\boldsymbol{x} - \boldsymbol{x}_{\boldsymbol{k}_i}\right\|\right) + \beta_1^z + \beta_2^z x + \beta_3^z y + \beta_4^z z \end{cases} \tag{8}$$

Radial basis method has several advantages that makes it very attractive in the area of mesh smoothing. The key point is that, being a meshless method, only grid points are moved regardless of element connected and it is suitable for parallel implementation. In fact, once the solution is known and shared in the memory of each calculation node of the cluster, each partition has the ability to smooth its nodes without taking care of what happens outside because the smoother is a global point function and the continuity at interfaces is implicitly guaranteed. Furthermore, despite its meshless nature, the method is able to exactly prescribe known deformations onto the surface mesh: this effect is achieved by using all the mesh nodes as RBF centres with prescribed displacements, including the simple zero field to guarantee that a surface is left untouched by the morphing action

4. LOAD MAPPING PROCEDURE

Figure 1 sketches the typical workflow of a steady FSI analysis based on coupling RANS and FEM solvers (sometime also called as 2-ways approach) [3]. The principle is to iterate between the two computations updating, in a closed loop, each configuration (the geometry for the CFD and the external loads for the FEM analyses). The two-directional connection between the two numerical domains is performed by the tasks of loads mapping and CFD mesh updating. The loads mapping consists in transferring the loads computed from the cells faces adjacent to the wall surfaces of the CFD configuration (integrating pressure and wall stress) to the correspondent points of the structural numerical domain in a form of force vectors. The mesh update consists in adapting the CFD

computational domain to the geometry deformation estimated by the structural analysis. The latter task is very efficiently performed applying mesh morphing techniques.

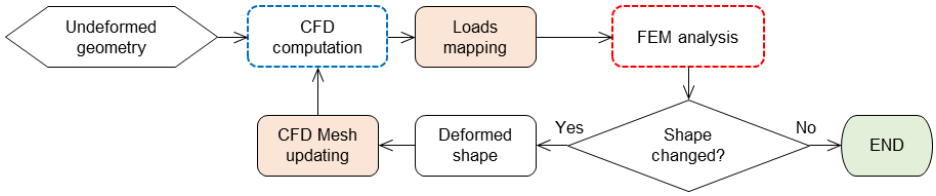

Figure 1: Workflow of a typical static CFD-CSM coupling procedure

Mapping methods must fulfil several requirements:

- **accuracy** - must be able to map vectors with minimum loss of modules and directions;
- **flexibility** - must be able to handle dissimilar meshes including fine-to-coarse and coarse-to-fine;
- **performance** - must be able to manage very large models in a reasonably short time.

The load mapping problem between non matching meshes (Figure 2) can be solved applying several methods. A review about load transfer schemes can be found in [4] and [5]. Practical examples in which aeronautical meshes are considered are presented in [6]. In the RIBES project, an approach combining several features of existing methods (pointwise, area weighted averaging, mortar elements), is proposed.

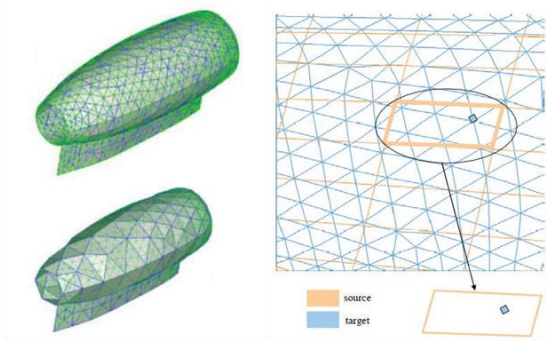

Figure 2: Example of mapping solutions thorough non-matching meshes

The procedure consists in decomposing the original datasets in small RBF problems. The field, defined as a set of values at the corresponding centroids or nodes of the source mesh, is interpolated by RBF. In case of force vectors field, the three components are interpolated by three independent RBF solutions. The Partition Of Unity (POU) method [7] is used to organize the source and target point sets into overlapping subdomains. In each subdomain the interpolation problem is locally solved and the force field exchanged between the source subdomain and its target counterpart. We finally obtain a set of local solutions that, in order to recover the continuity of the field, have to be combined together by blending functions. The smoothness of the global solution can be guaranteed by a polynomial blending function which is obtained from a set of smooth functions W_i by a normalization procedure:

$$w_i(x) = \frac{W_i(x)}{\sum_j W_j(x)} \tag{9}$$

where the condition $\sum W_i = 1$ has to be satisfied. The weighting functions W_i can be defined as the composition of a distance function D_i and a decay function V_i. The distance function has to satisfy the condition $D_i(x) = 1$ at the boundaries of a subdomain.
The shape of a subdomain can be arbitrarily chosen. For boxes subdomains the distance function assumes the simplest form:

$$D(x) = 1 - \prod_{r\in(x,y,z)} \frac{4(x_r - S_r)(T_r - x_r)}{(T_r - S_r)^2} \tag{10}$$

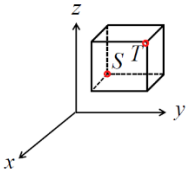

where S and T are the opposite points on the diagonal of the volume.
The forces on the target mesh nodes are obtained by multiplying the interpolated forces density field by the area (or volume for space fields) of the corresponding target cells. The error in the equilibrium between source and target field is related to this point and depends on the differences between the two discretization. A procedure able to smoothly recover the forces and moments equilibrium is then required. The goal is achieved introducing three corrective coefficients (one for each component along X, Y and Z) that locally force the equivalence between the resultants of the source and target subdomains (not necessarily equivalent to the subdomain used in the interpolation). The continuity and the smooth transition of the coefficients between the subdomains are obtained by overlapping them and by the adoption of blending functions with the same approach applied in the POU decomposition.
Assuming two overlapped subdomains, indicated as i and j, if the corrective coefficient set is constant within the same subdomain, the corrected resultants are obtained as:

$$\begin{cases} R_x = c_{x,i} \sum F_{x,i} w_i(x) + c_{x,j} \sum F_{x,j} w_j(x) \\ R_y = c_{y,i} \sum F_{y,i} w_i(x) + c_{y,j} \sum F_{y,j} w_j(x) \\ R_z = c_{z,i} \sum F_{z,i} w_i(x) + c_{z,j} \sum F_{z,j} w_j(x) \end{cases} \tag{11}$$

where the weight functions $w(x)$ are the same previously described.
The above formulations are valid for the computation of the homologous subdomain resultants if:

$$c_i = \begin{Bmatrix} 1 \\ 1 \\ 1 \end{Bmatrix};\ c_j = \begin{Bmatrix} 1 \\ 1 \\ 1 \end{Bmatrix} \tag{12}$$

This is due to the property that the blending functions sum identically sum to one, as mentioned above. The corrective coefficient for the selected subdomains are then expressed as:

$$\begin{aligned} c_{x,i} &= \frac{[\sum F_{x,i} w_i(x)]_{source}}{[\sum F_{x,i} w_i(x)]_{target}} & c_{x,j} &= \frac{[\sum F_{x,j} w_j(x)]_{source}}{[\sum F_{x,j} w_j(x)]_{target}} \\ c_{y,i} &= \frac{[\sum F_{y,i} w_i(x)]_{source}}{[\sum F_{y,i} w_i(x)]_{target}} & c_{y,j} &= \frac{[\sum F_{y,j} w_j(x)]_{source}}{[\sum F_{y,j} w_j(x)]_{target}} \\ c_{z,i} &= \frac{[\sum F_{z,i} w_i(x)]_{source}}{[\sum F_{z,i} w_i(x)]_{target}} & c_{z,j} &= \frac{[\sum F_{z,j} w_j(x)]_{source}}{[\sum F_{z,j} w_j(x)]_{target}} \end{aligned} \tag{13}$$

The reported correction is continuous and provides the mathematical equilibrium of local forces. It is then expected a low order of error on the moments.

4.1. Assessment of the load mapping procedure

The developed mapping procedure has been assessed using the HIRENASD (High Reynolds Number Aero-Structural Dynamics) test case. It consists in a half wing/fuselage wind tunnel model used in a workshop for aeroelastic numerical methods validation. Both CFD and FEM grids are then available. The static pressure field was mapped from the CFD wing surface grid to the wing structural FEM mesh. Table 2 reports the errors introduced by the interpolation process (without correction) between the two non-conformal domains.

Table 2: Errors of interpolation between the two non-conformal domains

$F_{x\,err}$ %	$F_{y\,err}$ %	$F_{z\,err}$ %	$M_{x\,err}$ %	$M_{y\,err}$ %	$M_{z\,err}$ %
47.3	6.6	1.0	13.1	13.8	27.8

The errors on forces and moments are significant especially on drag whose magnitude is in the order of 20 times lower than the lift.

Figure 3 and Figure 4 reports respectively the locations of the subdomains, by the positions of their centroids, and the map of the computed global correction coefficients obtained as:

$$\frac{\sqrt{(c_x A_x)^2 + \left(c_y A_y\right)^2 + (c_z A_z)^2}}{\sqrt{{A_x}^2 + {A_y}^2 + {A_z}^2}} \tag{14}$$

with A_i projected components of the nodal areas.
Table 3 reports the errors on moments (errors on forces are zero for definition) obtained with the correction procedure above described. The errors are below 1% along all directions.

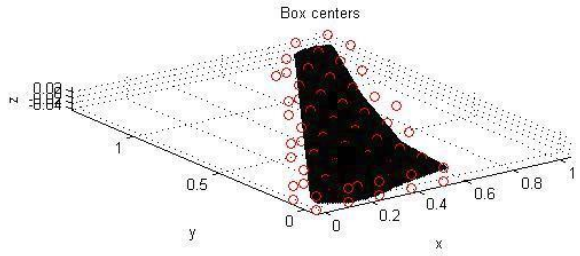

Figure 3: Map of subdomains centroids

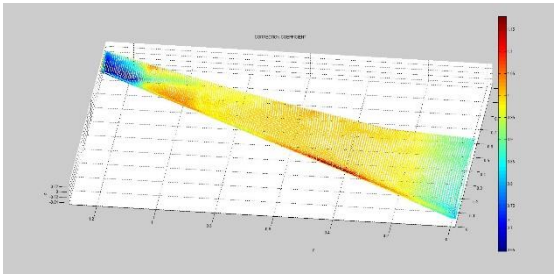

Figure 4: Map of global correction coefficients

Table 3: Errors of corrected interpolation

$M_{x\,err}$ %	$M_{y\,err}$ %	$M_{z\,err}$ %
0.8	0.11	0.38

5. EXPERIMENTAL CAMPAIGN

The accuracy of the developed load transfer numerical tools needs to be validated against a case of aeronautical interest. Such a test case should accomplish the task of being significant for a realistic design problem and of being suitable to be experimentally verified in a low speed wind tunnel (in order to contain the costs). The two objectives are conflicting in several practical aspects. An opportune compromise has then to be selected. The first requirement is accomplished developing a typical wing box structure referring to a realistic aircraft. The latter is achieved by an opportune aerodynamic design aimed to replicate as much as possible, at wind tunnel conditions, a realistic reference aircraft target load distribution.
In order to maximize the interaction between aerodynamic loads and wing deformation, a swept back wing is adopted[2]. Furthermore, to maximize the load similitude with a scaled wing model to be tested in a typical low speed facility, a relatively low wing load case has to be selected. With this vision, the wing is supposed to refer to a geometry suitable for an ultra-light jet class aircraft (Figure 5) whose possible realistic dimensions and performances are reported in Table 4.
The cruising lift coefficient is assumed to be 0.25. The relatively low Reynolds number allows adopting a laminar wing (the cruising Reynolds number is lower than 6 millions) whose pressure distribution should exhibit, for stability reasons, a slight favourable pressure gradient chordwise [9]. To not penalize the MMO conditions (maximum operating Mach number) the pressure recover should begin no later than 50-60% of the chord. Assuming a linear wing twist of 6 degree, the maximum section lift coefficient will be close to 0.4 in the inner region of the wing.

[2] The sweep angle introduces a coupling between aerodynamics and structural response because the deflection of the wing generates an aerodynamic twist variation [8].

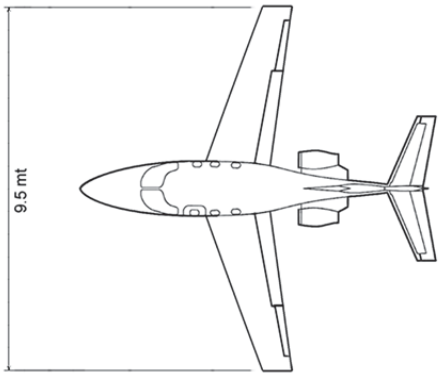

Figure 5: Reference aircraft configuration

Table 4: Reference aircraft data

Wing span	9.5 m
Reference wing surface	12 m^2
MTOW	2160 Kg
Service ceiling	41.000 ft
Cruise Mach number	0.75

Figure 6 reports a realistic target spanwise dimensionless (with root chord) load distribution and Figure 7 reports a typical transonic laminar airfoil target pressure distribution in cruising conditions. The wind tunnel model should be aerodynamically designed to replicate as much as possible these load shapes.

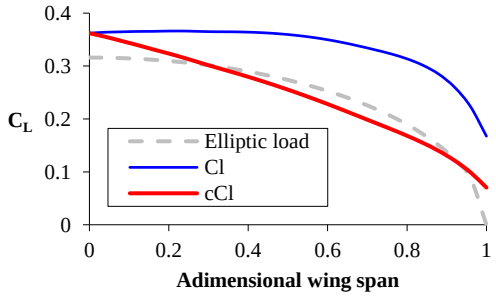

Figure 6: Spanwise load distribution

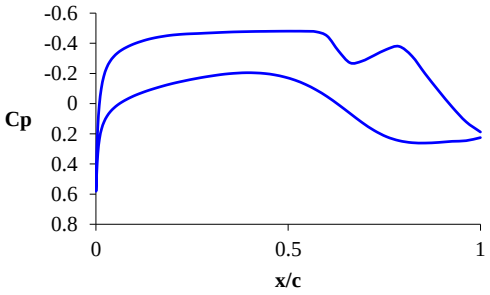

Figure 7: Laminar airfoil pressure distribution

5.1. Wing model design

A complete structural and load similitude at testing conditions would require a relatively high speed which is not compatible with a typical not pressurized low speed wind tunnel with a sufficient large test section[3]. The previously mentioned design compromise consists in accepting a lower model wing load, respect to the full-scale geometry, maintaining the similitude in the shape of the surface load distribution. The chosen scale of the model is 1:2.5 to which corresponds a span of 1.6 meters. Figure 8 and Table 5 detail the model geometry and its dimensions. Applying preliminary design methods [10], a total load of 45 Kg is expected to be generated at 40 m/s (Mach 0.12) with a lift coefficient close to 0.6 and a Reynolds number, referred to the model MAC (Mean Aerodynamic Chord), of 1.4 million. Such lift value correspond to a wing load of 60 Kg/m^2 which is approximately one fourth of the reference aircraft wing load.

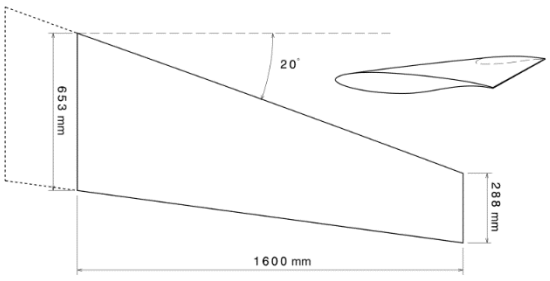

Figure 8: Wind tunnel model surface

Table 5: Model dimensions

Model scale	1:2.5
Span	1600 mm
Reference surface	0.754 m^2
MAC	495 mm
Root chord	653 mm
Tip chord	288 mm
Root thickness	85 mm
Tip thickness	29 mm
LE sweep angle	20°

[3] The speed required to generate a similar scaled load on a model with a span smaller than 2 meter, assuming the same full-scale aircraft wing load and design cruising lift coefficient, would be higher than Mach 0.3.

The wing will be installed on the side wall of the test section as a cantilever. The wet surface is generated by a loft built around the root and the tip airfoils. A single curvature surface is then generated. The two sections were aerodynamically designed to let the wing generate a load shape distribution, at low speed (Figure 9), similar to the typical pressure distribution generated by a laminar transonic wing in cruise conditions (Figure 7) but with a wing target 3D lift coefficient of 0.6. In the inner region, a local section Cl value of around 0.7 is then generated. Table 6 reports the target design point of the wind tunnel model and its thickness constraints.

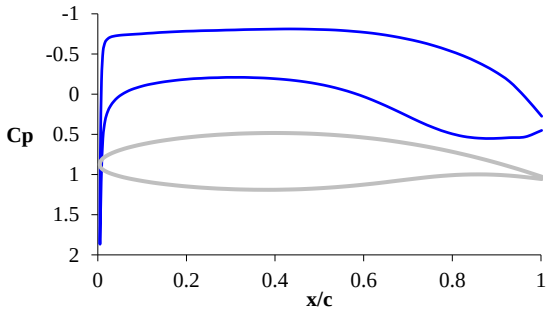

Figure 9: Target model section low speed pressure distribution

Table 6: Wind tunnel model targets of design

Design speed	40 m/s
Lift coefficient	0.6
Angle of attach	2°
Tip section thickness	10%c
Root section thickness	13%c

The model reproduces a typical metal aeronautical wing structure. The wing box is composed by two spars, at 10% and at 60% of the chord, and by ribs equally spaced (Figure 10). The external skin is divided into three parts: an upper, a lower and a leading edge panel. The lower panel is supposed to be joint by screws to allow an easy inspection of the internal installations while the other parts will be assembled by rivets.

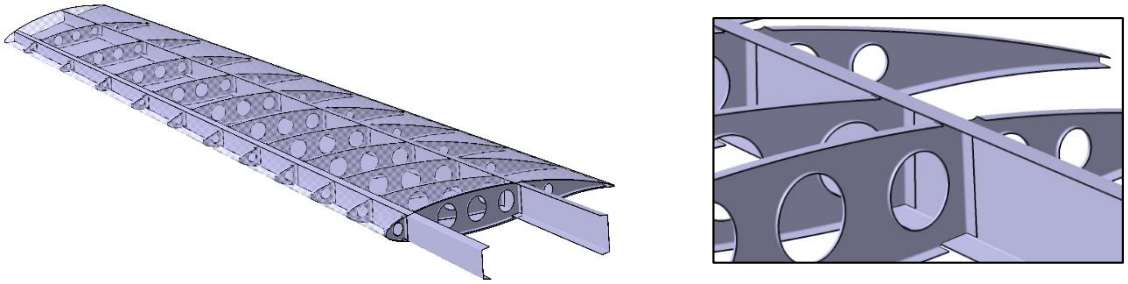

Figure 10: Structure of the wind tunnel model

Two lines of pressure taps will be installed at the 30% and at 70% of the model span. A number of 40 are planned to be located at the inner station, 25 at the outer and 15 spanwise on both upper and lower surface. Strain gauges will be positioned at several points on skin, spars and ribs in the most significant locations identified by the FEM analysis.

5.2. Wind tunnel tests

The wind tunnel tests will be performed in the facility of the university “Federico II” in Naples. It is a closed tunnel with a test section 2 meter wide and a maximum airflow speed of 45 m/s. It is equipped with balances whose measurement limits are 100 Kg for the lift and 20 Kg for the drag. The test matrix will cover a speed range from 35 to 45 m/s. Transition trips will be located at 5% of the chord on both sides of the model in order to guarantee a fully turbulent boundary layer and to reduce risks of separation. Lift, drag and pressure will be measured. Strain gauges measurements and deformation visualization will be reported at the most significant polar points. In order to verify if separations occur one polar will be measured applying mini tufts on the upper surface (Figure 11).
The model deformation will be evaluated, at the most significant test conditions, by photogrammetry techniques. The principle is to obtain a stereoscopic visualization by taking a couple of images

simultaneously using two cameras installed with different angle respect to the model [11]. The 3D geometric reconstruction process consists in recognizing the position of a matrix of markers, opportunely placed on the model surface, by the visual 3D evaluation of the displacement of this discrete number of points respect to their known static positions. The 3D coordinates of the points, in an absolute frame, are derived from their 2D location in the images according to the principle that every points are projected onto a particular point in the camera sensor plane and has to lie on a straight line (Figure 12).

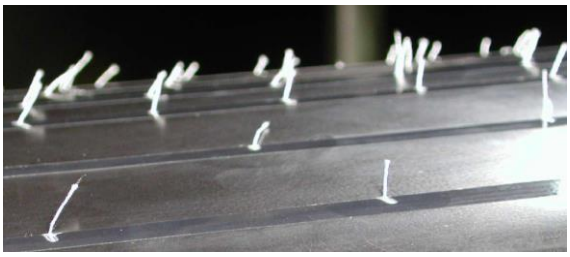

Figure 11: Mini tufts for flow visualization

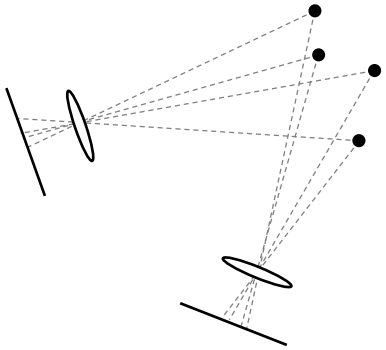

Figure 12: Principle of stereoscopic visualization

5.3. Preliminary CFD solutions

A set of preliminary CFD computations has been performed in order to verify the wing aerodynamic characteristics and to provide the load distribution required for the structural dimensioning. The fluid dynamic domain reproduced the tunnel test section including the inlet convergence element (Figure 13). The mesh was composed by 3.5 million of hexahedral elements. The boundary layer was solved up to the wall of the wing model while a wall function was applied to the tunnel walls. The complete fully turbulent polar was computed at the maximum velocity of 45 m/s to which correspond Mach 0.132 and Re 1.52 million (Figure 14). The wing is estimated to stall at 12 degree of incidence. The maximum lift conditions measurable by the balance occurs at around five degree of incidence in a region in which the lift polar is still linear.

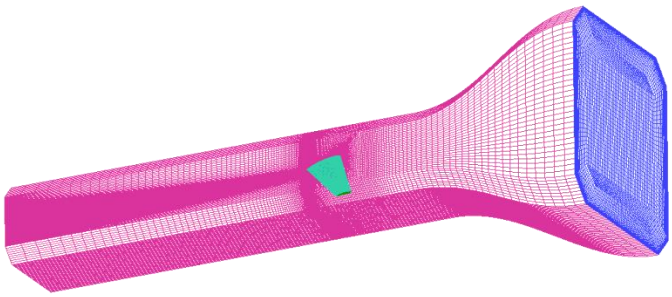

Figure 13: CFD domain reproducing the wind tunnel

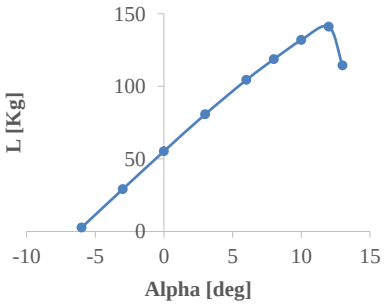

Figure 14: Computed wing lift curve

6. STRUCTURAL OPTIMIZATION ENVIRONMENT

Structural optimization is a strategic topic in aircraft design. The weight reduction is directly connected to the performances improvement and to the "green" behaviour of the machine. The safety margins, in particularly, play the leading role. The challenge is to acquire a total confidence on the numerical tools so to be able to move its values toward the unity all over the whole structure. Numerical optimizations coupled to structural analysis codes represent key strategies to get closer to this target.
The procedure developed in the RIBES project is based on routines that manage the geometric parameters, update the model, perform the FEM analysis and drive the optimization. The optimum selection criterion is based on filling a DOE (Design Of Experiment) table, in selecting the design points with the Latin hypercube sampling method [12], and on the application of a Response Surface (RS) on

which to apply the search algorithm. One of the most efficient approach, for the RS evaluation, is the Kriging method and the RBF interpolation [13]. The University of Rome "Tor Vergata" developed a Response Surface metamodel based on the Radial Basis Functions using various kernels.
The possibility to perform both a shape and thickness optimization was implemented by two different strategies. Thickness is introduced as variable of design directly taking the control of the bulk data file by the management of the property label in the ASCII file (Figure 15).

```
$ Femap with NX Nastran Property 1 : long. anteriore
PSHELL          1       6  0.0005         6               6               0.
$ Femap with NX Nastran Property 2 : long. posteriore
PSHELL          2       6 0.00067         6               6               0.
$ Femap with NX Nastran Property 3 : centina 1
PSHELL          3       6  0.0005         6               6               0.
$ Femap with NX Nastran Property 4 : centina 2
PSHELL          4       6 0.00051         6               6               0.
$ Femap with NX Nastran Property 5 : centina 3
PSHELL          5       6  0.0005         6               6               0.
```

Figure 15: Bulk data file

The shape change is applied to the topology directly on the numerical domain by mesh morphing techniques (Figure 16). The main advantages respect a CAD driven procedure are that no remesh is required (ensuring higher robustness) and the grid topology is maintained unchanged (no further uncertainness are introduced). The drawback is that a back-to-CAD procedure is required at the end of the optimization process. With mesh morphing, new shapes are generated by deforming the baseline mesh updating the nodal positions according to the prescribed geometric modification. Several algorithms have been explored for this task [14] [15]. One of the most efficient, which combines the benefits of a meshless method with a great precision, is based on the use of Radial Basis Functions interpolation [16] [17]. An additional advantage is that the RBF computation can be highly parallelizable. The process is then suitable to be implemented on HPC environment to manage very large computational domains. The first industrial implementation of RBF mesh morphing was introduced in 2009 with the software RBF Morph [18] (examples of applications can be found in [19]). The mesh morphing algorithm implemented in the RIBES software is based on its kernel.

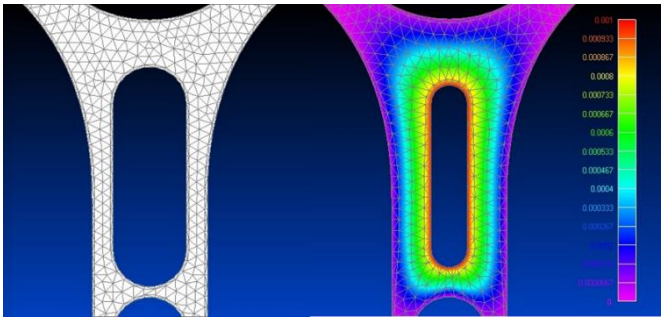

Figure 16: Example of shape parameterization based on mesh morphing

The shape modification is applied to the computational domain as a linear combination of vectors belonging to the FEM model nodal positions space.

$$X_{FEM} = X_{FEM0} + \sum_{s=1}^{n_{shapes}} \eta_s \delta X_s \tag{15}$$

The morphed FEM mesh is defined summing to the original grid nodes the displacements δX_s amplified by the shape parameters η_s. According to eq. (15) the optimization process is a shape optimizer that has the capability to involve parameters defined by the user and implemented in the setup of the model.
The complete workflow of the structural optimization procedure is sketched in Figure 17. The automatic process is included in the dashed frame while the external blocks indicate the setup activities that have to be performed in advance. E set of scripts routines drive the computation, extracts the solutions, formulate the objective functions, update the FEM setup according to the selected design point, complete the DOE table, compute the Response Surface and apply the single or multi objective search algorithm to find the optimum or the Pareto solution. The parameters that is possible to extract to be used to

compute the objective functions and/or implement constraints are the maximum stress, the maximum displacement (for the entire structure or for each property of the model) and the total mass of the structure.

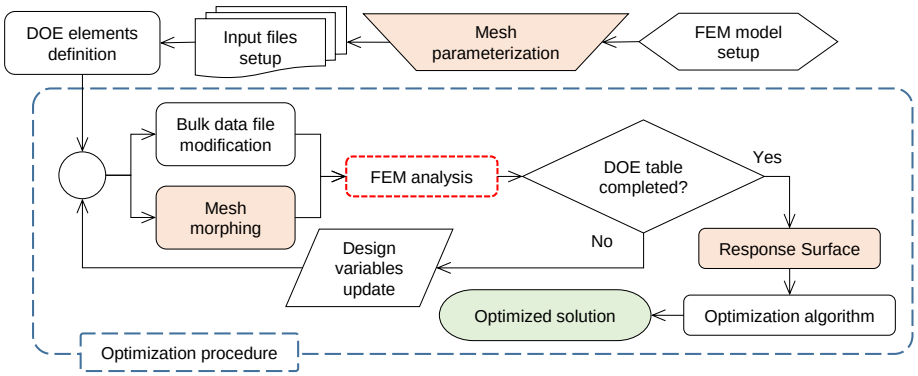

Figure 17: Optimization workflow

6.1. Procedure application on the test article

The wing structure developed for the wind tunnel test (Figure 10) and described in the previous paragraph was used as a test case to verify the optimization procedure. A two-objective optimization involving sheet metal thickness and rear spar caps shape was performed. The objective functions were the maximum stress and the total mass. Table 7 lists the six implemented variables of design. Two shape modifier factors were applied to the rear spar caps: a constant width variation and a linear tapering (Figure 18).

Table 7: Design variables

Skin thickness
Rear spar thickness
Front spar thickness
Ribs thickness
Rear spar caps tapering
Rear spar caps width

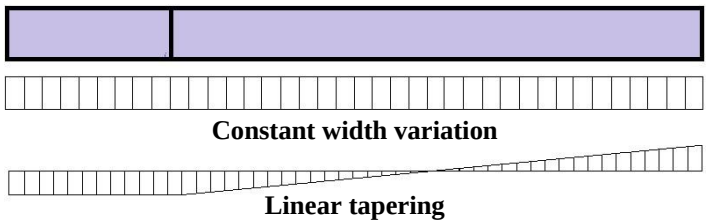

Figure 18: Spar caps shape modifiers

The DOE table was populated with 120 solutions. Figure 19 reports the Pareto frontier obtained. The optimum solution was chosen with the vision of significantly gain in terms of safety margins accepting a weight increment also respect to the baseline solution. Figure 20 compares the maximum stress obtained on the baseline configuration with the values obtained on the selected optimized structure configuration.

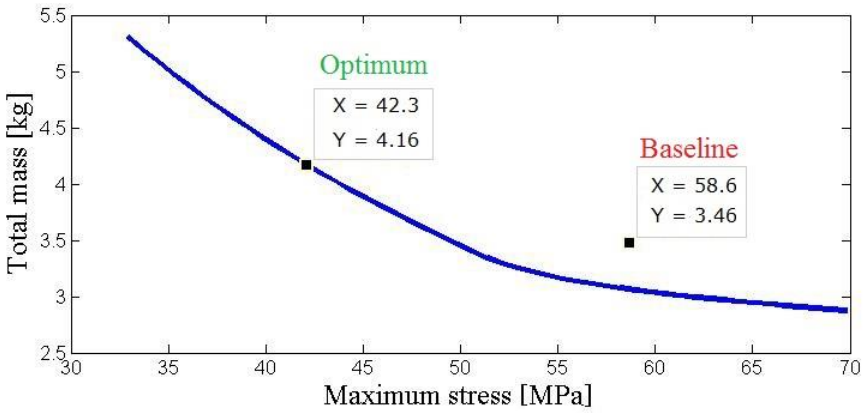

Figure 19: Pareto solution of the wing structure optimization

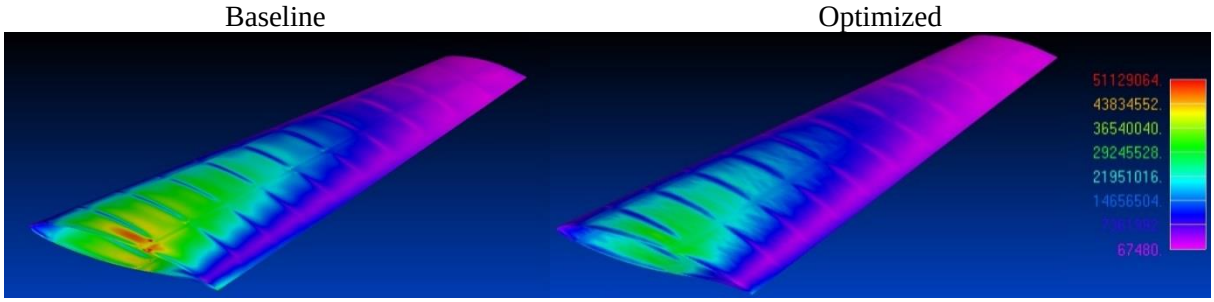

Figure 20: Maximum stress comparison between baseline and selected optimized solution

7. CONCLUSIONS

An overview of the activities performed within the "RIBES" EU research project, led by the University of Rome "Tor Vergata" and funded within the 7th framework aeronautics programme, was provided. Partners of research are the RBF Morph™ (www.rbf-morph.com) software vendor and the aerospace consulting engineering firm Design Methods™ (www.designmethods.aero). The project is aimed to the development of an accurate load mapping procedure suitable for Fluid Structure Interaction (FSI) analysis methods based on CFD-CSM coupling, to the setup of a shape structural optimization procedure and on the definition of an experimental campaign expressly customized for the validation of the software developed within the project.

An innovative mapping procedure, based on Radial Basis Functions, was implemented introducing corrective coefficients that smoothly recover the forces and moments equilibrium forcing the equivalence between the resultants of the source and target domains. The procedure was tested mapping the static pressure field from the CFD wing surface grid to the structural FEM mesh of the HIRENASD test case. The performances deriving from the application of the developed corrective factors were demonstrated by the reduction below 1% of the errors, introduced by the interpolation process between the two non-conformal domains, in the computation of the global moments.

The experimental campaign was setup with the requirement of being representative of a typical aeronautical wing structure. A half wing model, composed by ribs, spars and skin to be joint by rivets, was designed referring to an ultra-light jet class aircraft. The model will be equipped with pressure taps and strain gauges and will be tested in a non-pressurized low speed wind tunnel. The model deformation will be measure applying photogrammetry techniques.

A structural optimization procedure was developed by integrating a structural solver in a numerical optimization environment. A shape parameterization, based on RBF mesh morphing techniques, and a thickness control, was included in the procedure to be used as variables of design. The optimization criterion is based on filling a DOE table and on the computation of a Response Surface. The performance of the tool was demonstrated optimizing the wing structure designed for the experimental campaign.

BIBLIOGRAPHY

[1] Charles A. Micchelli, "*Interpolation of scattered data: Distance matrices and conditionally positive definite functions*". Constructive Approximation, Vol 2, Issue 1, pag. 11 – 22, 1996, doi: 10.1007/BF01893414.

[2] Armin Beckert and Holger Wendland, "*Multivariate interpolation for fluid-structure-interaction problems using radial basis functions*", Aerospace Science and Technology, Vol. 5, n. Issue 2, pag. 125 - 134, February 2001, doi: 10.1016/S1270-9638(00)01087-7.

[3] Ubaldo Cella and Marco Evangelos Biancolini, "*Aeroelastic Analysis of Aircraft Wind Tunnel Model Coupling Structural and Fluid Dynamic Computational Codes*", AIAA Journal of Aircraft, Vol. 49, n. 2, pag. 407 - 414, March - April 2012, doi: 10.2514/1.C031293.

[4] Xiangmin Jiao and Michael T. Heath, "*Common-refinement-based data transfer between non-matching meshes in multiphysics simulations*", International Journal For Numerical Methods In Engineering, Vol. 61, pag. 2402 - 2427, 2004, doi:10.1002/nme.1147.

[5] R.K. Jaiman, X. Jiao, P.H. Geubelle, E. Loth, "*Conservative load transfer along curved fluid–solid interface with non-matching meshes*", Journal of Computational Physics, Vol. 218, n. 1, pag. 372 - 397, October 2006, doi:10.1016/j.jcp.2006.11.029.

[6] Jamshid Samareh, "*Discrete Data Transfer Technique for Fluid-Structure Interaction*", 18th AIAA Computational Fluid Dynamics Conference, June 2007, doi:10.2514/6.2007-4309.

[7] I. Babuška and J. M Melenk, "*The Partition of Unity Method*", International Journal for Numerical Methods in Engineering, Vol. 40, Issue 4, pag. 727 – 758, February 1997, doi: 10.1002/(SICI)1097-0207(19970228)40:4<727::AID-NME86>3.0.CO;2-N.

[8] Daniel P. Raymer, "*Aircraft Design: A Conceptual Approach*", 3rd ed., AIAA Education Series, NewYork (NY), 1999.

[9] Ubaldo Cella, Domenico Quagliarella, Raffaele Donelli and Biagio Imperatore, "*Design and Test of the UW-5006 Transonic Natural-Laminar-Flow Wing*", AIAA Journal of Aircraft, Vol. 47, n. 3, pag. 783 - 795, May - June 2010, doi: 10.2514/1.40932.

[10] J. Roskam and C. T. E. Lan, "*Airplane Aerodynamics and Performance*", DARcorporation, Lawrence, KS, 1997.

[11] F. Fossati, R. Sala, A. Basso, M.Galimberti D. Rocchi, "*A multicamera displacement measurement system for wind engineering testing*", EACWE 5, Florence (Italy), 19 - 23 July 2009.

[12] M. D. McKay, R. J. Beckman and W. J. Conover, "*A Comparison of Three Methods for Selecting Values of Input Variables in the Analysis of Output from a Computer Code*", Technometrics, Vol. 21, n. 2, pag. 239 – 245, doi: 10.2307/1268522.

[13] R. Jin, W. Chen, T.W. Simpson, "*Comparative studies of metamodelling techniques under multiple modelling criteria*", Structural and Multidisciplinary Optimization, Vol. 23, n. 1, pag. 1 - 13, December 2001, doi:10.1007/s00158-001-0160-4.

[14] T. W. Sederberg and S. R. Parry, "*Free-Form Deformation of Solid Geometric Models*", proceedings of the 13th Annual Conference on Computer Graphics and Interactive Techniques (SIGGRAPH 86), David C. Evans and Russell J. Athay (Eds.). ACM, New York, NY, USA, pag. 151 – 160, 1986.

[15] A. Masud, M. Bhanabhagvanwala, R. A. Khurram, "*An Adaptive Mesh Rezoning Scheme for Moving Boundary Flows and Fluid-Structure Interaction*", Computers and Fluids, Vol. 36, n. 1, pag. 77 - 91, January 2007

[16] A. de Boer, M.S. van der Schoot, H. Bijl, "*Mesh Deformation Based on Radial Basis Function Interpolation*", Computers and Structures, Vol. 85, Issues 11 - 14, June - July 2007, pag. 784 - 795, doi:10.1016/j.compstruc.2007.01.013.

[17] S. Jakobsson and O. Amoignon, "*Mesh Deformation using Radial Basis Functions for Gradient Based Aerodynamic Shape Optimization*", Computers and Fluids, Vol. 36, Issues 6, July 2007, pag. 1119 - 1136, doi:10.1016/j.compfluid.2006.11.002.

[18] Marco Evangelos Biancolini, "Mesh Morphing and Smoothing by Means of Radial Basis Functions (RBF): A Practical Example Using Fluent and RBF Morph", Handbook of Research on Computational Science and Engineering: Theory and Practice, IGI Global, 2012, ISBN13: 9781613501160.

[19] A. Khondge and S. Sovani, "*An Accurate, Extensive, and Rapid Method for Aerodynamics Optimization: The 50:50:50 Method*", SAE Technical Paper, 2012-01-0174, doi:10.4271/2012-01-0174.